NJC

ROYAL SOCIETY OF CHEMISTRY

PAPER

View Article Online
View Journal | View Issue

Cite this: *New J. Chem.*, 2023, **47**, 18485

Unusual tellurium(IV) mediated cyclisation diols into dihydroxazoles with potential anticancer activity†

Kenneth D'Arcy,‡[a] Tim Schäfer,‡[a] Michele De Franco,[b] Raffaele Ricco,*[c] Valentina Gandin,[b] Pablo J. Sanz Miguel[d] and Diego Montagner*[a]

Received 7th July 2023,
Accepted 21st September 2023

DOI: 10.1039/d3nj03186a

rsc.li/njc

The role of tellurium in medicinal chemistry has recently grown in importance due to the discovery of the anticancer properties of SAS and AS-101, two inorganic compounds based on Te(IV). Here we describe an unprecedented isolation of a series of tetramethyl-dihydroxazole tellurium hexachloride salts whose structure has been indentified and characterised with several techniques including X-ray crystallography. The novelty resides on the role of tellurium that mediate the cyclisation of 1,1,2,2-tetramethylethylene into duhydroxazole in the presence of nitriles. Reaction mechanism, physiological stability and preliminary cytotoxicity results are discussed.

Introduction

The peculiar metalloid nature of tellurium allows for the formation of a variety of compounds with different oxidation states, from −2 to +6, although the predominant complexes occurring in both inorganic and organometallic species show an oxidation state +4.[1] Some tellurium compounds have shown to express specific biological activities, for example alkali metal tellurites and tellurates show antibacterial activity, organotellurides and diorganoditellurides have potent antioxidant activity, while inorganic and organic tellurium compounds are effective inhibitors of caspase and cathepsin proteases.[2–7]

At present, only two inorganic tellurium(IV) compounds have been studied for their anti-cancer properties: ammonium trichloro(dioxoethylene-*O*,*O*′)tellurate (AS-101) and octa-*O*-bis-(*R*,*R*)-tartarate ditellurane (SAS) (Fig. 1).[8–15]

Between them, AS-101 has shown a variety of potential therapeutic applications thanks to its potent immune-modulatory action both *in vitro* and *in vivo*,[10] making it a good trial candidate for phase I and phase II clinical studies with cancer patients. Its biological activities primarily results from the specificity of Te(IV) as redox-modulator, inactivating cysteine proteases such as cathepsin B, inhibiting specific tumour survival proteins such as survivin, and obstructing the production of tumoral Interleukin-10 (IL-10), an anti-inflammatory cytokine also known as human cytokine synthesis inhibitory factor (CSIF).[12]

Most of these properties have direct influence on anti-cancer activity or sensitization of tumours to chemotherapy. Along with these properties, inorganic Te(IV) compounds such as SAS and AS-101 showed excellent safety profiles, holding much promise as anti-cancer therapeuticals.[15–18] Recently, our group reported the synthesis and characterisation of a series of AS-101 analogues (structure **A** in Fig. 1) by introducing additional functional groups on one of the two carbons of the vicinal diol ligand.[19] The novel complexes showed different stability depending on the alkyl substituents and demonstrated interesting antimicrobial activity.[19] With the aim of expanding the library of this class of compounds and determining how the functionalisation of the glycol moiety would affect the biological

[a] *Department of Chemistry, Maynooth University, Ireland. E-mail: diego.montagner@mu.ie*
[b] *Department of Pharmaceutical and Pharmacological Sciences, University of Padua, Italy*
[c] *Department of Industrial Systems Engineering, Asian Institute of Technology, Thailand*
[d] *Departamento de Química Inorgánica, Instituto de Síntesis Química y Catálisis Homogénea (ISQCH), Universidad de Zaragoza-CSIC, 50009 Zaragoza, Spain*

† Electronic supplementary information (ESI) available. CCDC 2263654, 2271363 and 2263653. For ESI and crystallographic data in CIF or other electronic format see DOI: https://doi.org/10.1039/d3nj03186a

‡ These authors contributed equally to the research presented in this manuscript.

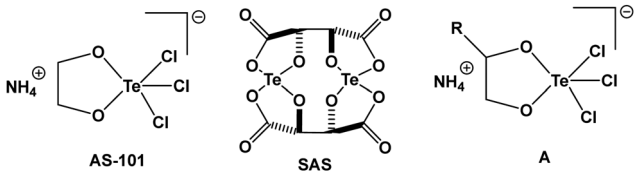

Fig. 1 Structure of tellurium (IV) compounds: AS101 (Ammonium trichloro(dioxoethylene-*O*,*O*′)tellurate); SAS (octa-*O*-Bis-(*R*,*R*)-tartarate ditellurane) and analogues of AS-101 (**A**) previously reported by us.[19]

properties, we started to use vicinal diol ligands bearing functional groups on both carbons. Surprisingly, when pinacol (1,1,2,2-tetramethylethylene glycol), that carries for methyl groups, was used in the previously reported synthetic procedure using acetonitrile as solvent,[19] we isolated a completely new salt species of $TeCl_6^{2-}$ with an oxazole cation.

Encouraged by this unexpected result, three novel compounds were synthesised and characterised by multinuclear NMR, IR, mass, elem. Analys. and X-ray diffraction. The mechanism of decomposition in water was determined and the most stable compound was screened as anticancer agent with very promising activity against three cancer cell lines.

Results and discussion

Synthesis and characterisation

The analogues of AS-101 compounds recently reported by us (structure **A** in Fig. 1) were synthesised by refluxing the corresponding diol with $TeCl_4$ in anhydrous acetonitrile.[19]

In details, we used pinacol as diol under reflux for five hours, expecting to obtain a compound with the same structure of $\mathbf{A_1}$ (Scheme 1). After cooling down the solution at room temperature, the addition of diethyl ether (Et_2O) resulted in the precipitation of a white powder. Unfortunately, neither the ^1H and ^{13}C NMR spectra nor the elemental analyses (see ESI†) matched with the expected structure $\mathbf{A_1}$. Slow diffusion of diethyl ether into an acetonitrile solution of the white compound, afforded nice yellow crystals whose structure was determined by X-ray diffraction, as discussed later. The compound was found to be a salt in which the organic cationic part is an oxazole ligand derived from the condensation and cyclisation between pinacol and acetonitrile, while the counter anion contains tellurium as $TeCl_6^{2-}$ (**1**, Scheme 1).

The reaction to produce compound **1**, as described in Scheme 1, is not stoichiometric due to the initial 1 : 1 ratio between diol and Te(IV) species, therefore a side product is expected. In-depth FTIR characterisation and Elem. Analysis confirmed the presence of the additional species [TeO_2·2HCl, **B**], Indeed, the white compound isolated after precipitation with diethyl-ether, shows an Elem. anal. which closely matched with the mixture of **1** and **B** (El. anal. calcd for **1** + **B**, $C_{16}H_{34}Cl_8N_2O_4Te_2$ (%): C: 22.42; H: 4.00; N: 3.27. Found C: 22.12; H: 4.23; N: 3.47). Therefore, the reaction is found to proceed as shown in Scheme 2, with TeO_2·2HCl indicated as (**B**) as a side product.

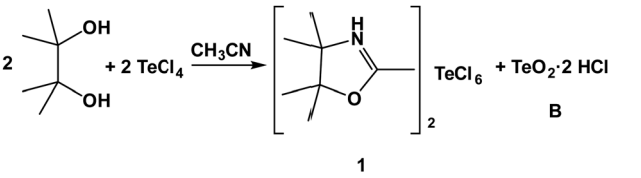

Scheme 2 Stoichiometric pathway for the synthesis of **1** + **B**.

Compound **1** can be separated as a pure yellow solid as described in the Experimental section.

Noteworthy, the same mixture **1** + **B** is obtained by varying the stoichiometric ratio between $TeCl_4$ and pinacol. We hypothesize that the formation of the 2-oxazoline salt **1** may proceed *via* two similar pathways, reported in Scheme 3. The first is a Pinner reaction, according to the left side of Scheme 3.[20,21]

In this instance, the nitrile initially reacts with $TeCl_4$, weakening the triple bond, which now can be subject to an attack by one of the two OH groups of the pinacol. The intermediate, $TeCl_4$-stabilized, amidinium ion loses one molecule of water

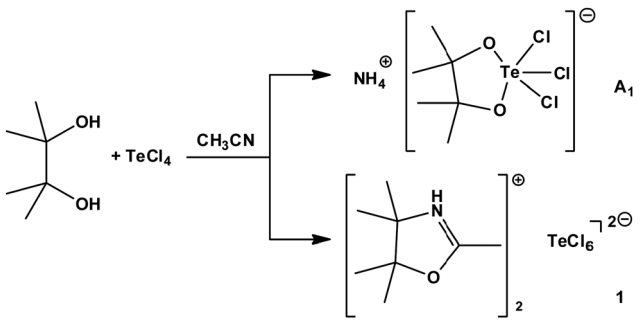

Scheme 1 Synthetic route for the production of **1**. The upper pathway represents the expected result ($\mathbf{A_1}$), the lower pathway represents the actual product obtained (**1**).

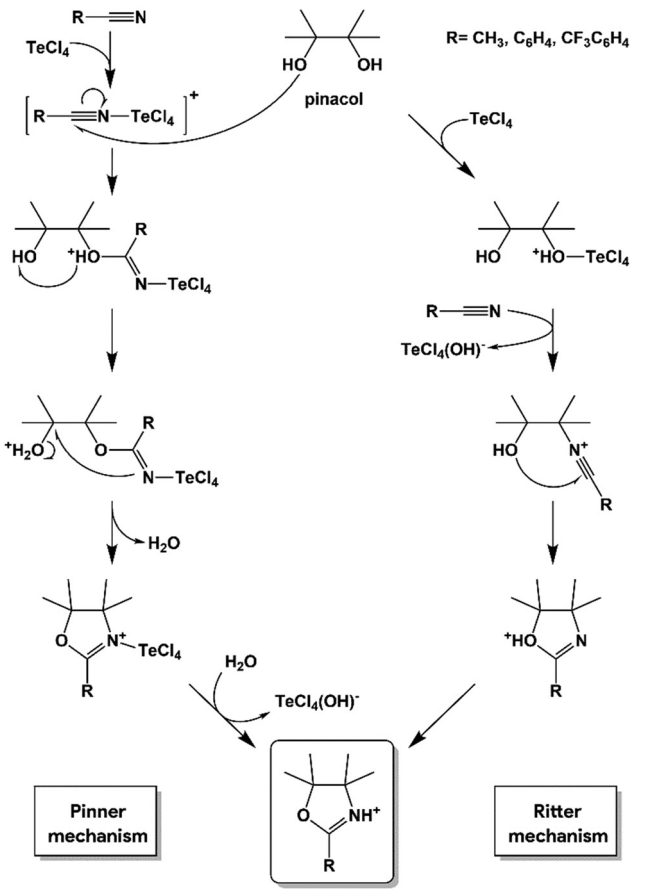

Scheme 3 Proposed pathways for the production of the tetramethyloxazolium (TMO) cation of **1**. Left: the Pinner mechanism; Right: the Ritter mechanism.

from the vicinal alcohol, with a transient formation of a carbenium ion (not shown) and immediate cyclization into the 2-oxazoline. The liberated water molecule can react again with the tetramethyloxazolium (TMO)-$TeCl_4$ intermediate, forming an equivalent of $TeCl_4(OH)^-$ and a proton, which is likely to protonate back the TMO on the nitrogen.

An alternate, concurrently occurring, mechanism for the formation of TMO invokes a modified Ritter reaction, according to the right side of Scheme 3.[22,23] Initially, $TeCl_4$ reacts with one OH group from the pinacol. This derivative quickly reacts with the excess nitrile species, resulting in the formation of the $TeCl_4(OH)^-$ species and a nitrilium ion that undergoes cyclization by the action of the vicinal OH group of the pinacol, forming a *O*-protonated TMO, readily tautomerizing into the desired *N*-protonated TMO.

In any case, the resulting $TeCl_4(OH)^-$ will form $TeCl_2(OH)_2$ and $TeCl_6^{2-}$ according to the reactions:[24]

$$2TeCl_4(OH)^- \rightarrow TeCl_2(OH)_2 + TeCl_6^{2-}$$

$$TeCl_2(OH)_2 \rightarrow TeO_2 + 2HCl$$

The former then further hydrolyses to TeO_2 + 2HCl, whereas the latter acts as counterion of the two generated equivalents of TMO.

After this intriguing result, we tried to use different nitriles, isolating analogues compounds when acetonitrile is replaced with benzonitrile (**2**) or 4-(trifluoromethyl)benzonitrile (**3**). The novel compounds are fully characterised by mono and bidimensional ^1H, ^{13}C, ^{125}Te NMR, mass spectrometry, IR, elemental analyses and X-ray diffraction (see Experimental and ESI† sections). Interestingly, the same species are not formed with other nitriles such as 3-trichloroacetonitrile, cyclohexanecarbonitrile or 1-naphthonitrile.

Pinacol and $TeCl_4$ are both essentials in the formation of these new species. By either replacing the former with other bis-substituted vicinal diols (*i.e.*, 1,1,2,2-tetraphenyl-1,2-ethanediol, catechol, hexafluoro-2,3-bis(trifluoromethyl)-2,3-butanediol and 2,3-butandiol), or the latter with $ZnCl_2$, $AlCl_3$ and $MgCl_2$, no evidence of the production of the same products is observed. It is likely that the carbocation arising from the removal of one OH groups of the pinacol, hypothesized (not shown) in Scheme 3, is instrumental to formation of the oxazoline, therefore excluding the feasibility of the reaction either with catechols (which would form highly unstable benzenium species) or secondary alcohols, (*e.g.* butanediol), whose carbenium ions would be less stabilized than the tertiary ones arising from the pinacol. Additionally, the utilization of sterically hindered diols (such as with phenyl groups), although interesting for the stabilization of a carbenium, can prevent or reduce the probability of attack on either the Te-activated nitrilium in the proposed Pinner mechanism, or from the nitrile in the Ritter mechanism. Finally, strongly electronegative groups (*i.e.*, perfluorinated ones) attached on the diol would not allow for a stable carbenium formation. Henceforth, the proposed mechanism could be reasonable on the basis of the unsuitability of the above-mentioned alternative reactants. It is also expected the Pinner mechanism (Scheme 3, left) to play a major role over the Ritter one (Scheme 3, right), given the high amount of nitrile in the reaction mixture. However, a resolutive answer in this view could only be sought through accurate mechanistic studies, which go beyond the scope of this research.

Compounds **1**, **2**, and **3** were thoroughly characterized by X-ray crystallography. Slow diffusion of Et_2O into dimethylformamide (DMF) solutions of **1**, **2**, and **3** yielded the respective salts $[CH_3TMO]_2[TeCl_6]\cdot 2DMF$ (TMO = 4,4,5,5-tetramethyloxazolium) (**1**·2DMF), $[PhTMO]_2[TeCl_6]\cdot 2DMF$ (**2**·2DMF), and $[(p\text{-}CF_3Ph)TMO]_2[TeCl_6]$ (**3**). Interestingly, the latter (**3**) does not crystallize as a solvate. Fig. 2 shows the structure of cations **1**, **2**, and **3** and the $[TeCl_6]^{2-}$ anion of compound **2**. Table 1 lists selected bond separations and angles for **1**, **2** and **3**.

In the crystal structure of **1**·2DMF, Te(IV) ion is located at the crystallographic inversion centre, and displays usual bond distances (Te1–Cl1, 2.5431(4) Å; Te1–Cl2, 2.5380(4) Å; Te1–Cl3, 2.5494(4) Å) and angles (maximal deviation from right angle: Cl2–Te1–Cl3, 91.102(13)°). The N4 site of the oxazole ring is protonated, and widening of the C3–N4–C5 angle is observed: 111.31(12)°. In addition, the O1–C2–C3–N4 torsion angle was found to be 23.32(12)°, which is probably a consequence of the steric accommodation of the four methyl substituents at the endocyclic C4–C5 bond. The separation between the endocyclic C5 site and the methyl group is 1.477(2) Å. Regarding the crystal packing, the N4(H) site is involved in hydrogen bonding with the oxygen atom of a neighbouring DMF molecule (2.6872(16) Å).

Analogously, the structure of **2**·2DMF exhibits the typical geometry of the $[TeCl_6]^{2-}$ anion (Table 1), and the resulting geometry of the $[PhTMO]^+$ cation is similar to that of **1**, except for the presence of the Ph– unit. The O1–C2–C3–N4 twist angle is 23.32(10)°. Distance between the C5 site and C11(Ph) (1.4596(15) Å) is slightly shorter to that of **1**·2DMF. The N4(H) site is connected *via* hydrogen bonding to an oxygen atom of the solvating DMF (2.678(1) Å).

Geometry of cation $[(p\text{-}CF_3Ph)TMO]^+$ (**3**) is similar to those of **1** and **2**, except for the substituent at the C2 position. Two Te–Cl

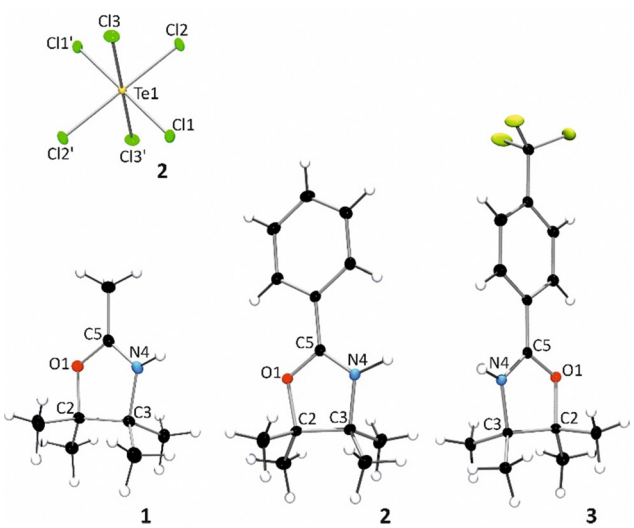

Fig. 2 View of a $[TeCl_6]^{2-}$ anion and the cations of **1**, **2**, and **3**.

Table 1 Selected endocyclic ring angles [°] and distances [Å] of cations of **1**, **2** and **3**

	1	**2**	**3**
Te1–Cl1	2.5431(4)	2.4557(4)	2.5271(3)
Te1–Cl2	2.5380(4)	2.5341(4)	2.5464(3)
Te1–Cl3	2.5494(4)	2.6432(4)	2.5385(3)
O1–C2	1.5111(17)	1.5063(15)	1.5035(13)
C2–C3	1.5577(19)	1.5548(18)	1.5609(16)
C3–N4	1.4817(17)	1.4938(16)	1.4841(14)
N4–C5	1.2887(19)	1.2953(17)	1.2946(15)
O1–C5	1.3191(17)	1.3138(16)	1.3120(14)
C5–O1–C2	107.36(10)	107.31(10)	107.67(9)
O1–C2–C3	101.41(10)	101.38(9)	101.46(9)
N4–C3–C2	99.64(11)	98.66(9)	99.61(9)
C5–N4–C3	111.31(12)	110.72(11)	110.79(10)
N4–C5–O1	114.03(13)	113.77(12)	114.25(10)

distances of the anion differ significantly from those observed in **1** and **2**, whereas bond angles remain unaltered (Table 1). As in the case of **1** and **2**, cation **3** exhibits a wide C3–N4–C5 angle (110.72(11)°) and a pronounced O1–C2–C3–N4 twist angle (26.64(11)°). The intramolecular hydrogen bonding pattern could be responsible for the hexafluorotellurate anion distortion, the N4(H) is connected *via* hydrogen bonding with a Cl3 ligand (N4(H)···Cl3, 3.2495(12) Å). Thus, each $TeCl_6^{2-}$ anion is connected to two CF_3PhTMO^+ cations.

Considering the poor stability exhibited by analogous compounds **A** (Fig. 1), an assessment was performed to evaluate the behaviour of compounds **1–3** in aqueous conditions. Briefly, the compounds were dissolved in pure water and stirred at r.t. for 72 hours; the solutions were dried under vacuum and the resulting samples analysed *via* ^{1}H and ^{13}C NMR in DMSO-d_6.

All the three compounds decomposed with different extent and the products showed a ^{1}H and ^{13}C NMR spectra with a similar pattern of the original species (see ESI†), indicating that the decomposition product must have a similar structure of the starting compounds. The percentage of the decomposition is roughly determined through the ^{1}H-NMR integrals and the data are reported on Table 2.

The hydrolysis of oxazoline derivatives in the presence of water is generally accepted to proceed *via* a ring open reaction (Scheme 4)[25] initiated by the attack of water at the C2 site of the oxazoline, forming the intermediate (**4**). The evolution is pH-dependent, and subsequent protonation can occur either at the *O* (pathway A), or at the *N* (pathway B). In the first case, a *N*-(3-hydroxy-2,3-dimethylbutan-2-yl) amide (**1a**) is formed, whereas a 3-amino-2,3-dimethylbutan-2-yl acylate (**1b**) is obtained in the second case (which can also be further protonated at the terminal amine producing **1c**).

Table 2 % of decomposition of compounds **1–3** after 72 h in aqueous solution

Compound	Decomposition (%)
1	9
2	40
3	92

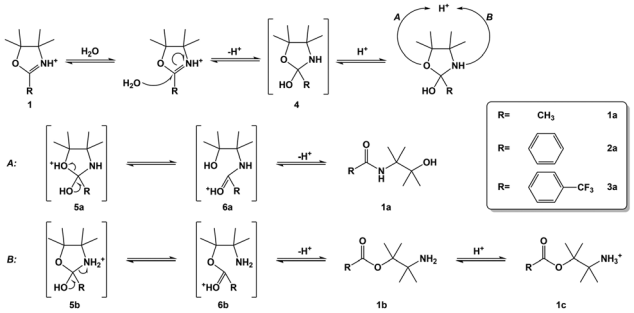

Scheme 4 The decomposition pathway of oxazoline derived from compound **1** ($TeCl_6^-$ not shown for clarity).

Notwithstanding, Greenhalgh *et al.*[26] have demonstrated how **1b** can further attack the protonated oxazoline **1** to produce **7a**, which hydrolyses to the amidate intermediate **8a** (Scheme 5). Considering that pure water is known to quickly adsorb atmospheric CO_2 producing a slightly acidic pH, this amidate is not fully stable also at mild pH values, therefore it can hydrolyse to produce additional **1a** and **1b**, the latter closing the loop. In summary, **1b** can act as a mediator for the oxazoline decomposition to amide **1a** in water.

The overall rate of decomposition depends on the EWG (electro-withdrawing-group) nature of the substituents in the oxazoline ring, as proposed by Moloney.[27] In line with this study, compound **3**, having a strong EWG (p-C_6H_4-CF_3), results the most unstable of the series, with more than 90% of decomposition after 72 hours; conversely, compound **1** results to be the most stable of the series with only 9% decomposition in the same timeframe. This observation further corroborates the above-mentioned ^{1}H-NMR study.

The formation of the decomposed products **2a** and **3a** is confirmed by LC-MS, with a peak (m/z) at 222 for **2a** and at 290 for **3a**. Due to the low degree of decomposition of **1**, the signal of **1a** was too low to be detected by the instrument. Further confirmations of this decomposition reaction mechanism are the strongly acidic conditions of the mixture (pH = 0) and the formation of TeO_2 as white powder precipitate after isolation from methanol.

Anticancer activity

Due to the low stability in aqueous conditions of compounds **2** and **3**, only compound **1** was kept for a biological screen.

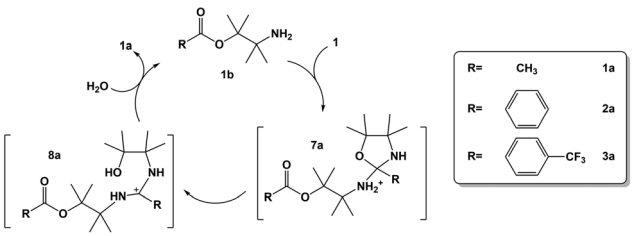

Scheme 5 Further decomposition of oxazoline into amide **1a** (and analogues **2a** and **3a**) mediated by the ester **1b** (and its aromatic analogues).

Table 3 *In vitro* antitumor activity of compound **1** tested in 2D cell cultures using cisplatin as control. Cells ($3–8 \times 10^3$ mL^{-1}). Cells were treated for 72 h with increasing concentrations of the tested compounds. The cytotoxicity was assessed by the MTT test and each experiment repeated three times. IC_{50} values (expressed as μM) were calculated by a four-parameter logistic model 4-PL ($p < 0.05$)

Cell line	**1**	Cisplatin
2008	1.25 ± 0.36	2.22 ± 0.81
LoVo Ox-Pt	1.18 ± 0.41	9.15 ± 1.92
PSN-1	7.58 ± 1.94	18.25 ± 3.11
H157	2.25 ± 0.85	3.9 ± 1.10

The anticancer property of **1** was studied on a panel of four cancer cell lines, 200 (ovarian), LoVo Ox-Pt (Colorectal oxaliplatin resistant); PSN-1 (Pancreatic) and H-157 (Lung) and the IC_{50} values are reported in Table 3.

Compound **1** showed very promising activity against all the tested lines, better than the reference cisplatin in most of the cases, demonstrating also to overpass resistance associated with platinum treatment.

The mechanism of action must be elucidated in detail and will be matter of a further publication, but a preliminary screening can exclude that thioredoxin reductase would be a suitable target as it happens for the most compounds containing selenium or tellurium that showed to hamper TrxR activity.[28–30]

Conclusions

Three novel dihydroxazole tellurium hexachloride salts were synthesised, fully characterised and preliminary screened as anticancer compounds. The compounds are formed by a cyclisation reaction of pinacol in nitrile solution mediated by $TeCl_4$. Reaction mechanisms are proposed corroborated with experimental data and crystal suitable for X-ray study were obtained for all the three compounds. The stability of the compounds was assessed in aqueous solution and only one of the compounds results stable to perform preliminary anticancer studies. The mechanism of decomposition is discussed and analysed *via* NMR. Due to the exotic nature of these compounds and to the interesting biological results obtained, we aim to enhance the library of these novel Te(IV) containing species and understand the mechanism of action with more detailed biological assays.

Experimental

Materials and methods

All reagents, solvents and reactants were purchased from commercial sources (Sigma-Aldrich and Flourochem) and used without further purification unless specified.

Elemental analyses (carbon, hydrogen and nitrogen) were performed with a PerkinElmer 2400 series II analyser. Infrared (IR) spectrometry was conducted on a PerkinElmer Spectrum 100 FT-IR. Attenuated Total Reflectance Fourier transform Infrared (ATR-FTIR) spectra were taken in the region 4000 cm^{-1} to 650 cm^{-1}, using 4 scans with a resolution of 4 cm^{-1}. NMR analyses were conducted with a Bruker Avance spectrometer at 500 MHz for ^1H, 126 MHz for ^{13}C, 158 MHz for ^{125}Te and 470 MHz for ^{19}F nuclei. Spectra were recorded in DMSO-d_6 using tetramethyl silane (Me_4Si) as the internal standard for ^1H and ^{13}C while diphenyl ditelluride (Ph_2Te_2) was used as external reference for ^{125}Te. All chemical shifts δ are reported in ppm. LC-MS was performed on an Agilent Technologies 1200 Series instrument consisting of a G1322A Quaternary pump and a G1314B UV detector (254 nm) coupled to an Advion Expression L Compact Mass spectrometer (ESI) operating in positive mode.

Crystallography. Crystal structure determination of complexes **1**, **2** and **3**. Data were collected with an APEX DUO Bruker (**1**, **3**) and a Bruker D8 Venture (2) diffractometers, by graphite-monochromated Mo Kα radiation (λ = 0.71073 Å). Single crystals were mounted on a fibre and coated with perfluoropolyether oil. Diffracted intensities were integrated with SAINT,[31] and corrected of absorption effects was performed with a multi-scan strategy by SADABS,[32,33] both programs integrated in the APEX2 package. Both structures were solved by direct methods with the software SHELXS[34] and refined by full-matrix least squares on F^2 with SHELXL,[35] and the WinGX system.[36]

Structural data for $[CH_3TMO]_2[TeCl_6]\cdot 2DMF$ (**1**·2DMF): $[C_{22}H_{46}Cl_6N_4O_4Te]$, M_r = 770.93, yellow block, orthorhombic *Pbca*, a = 15.5390(14) Å, b = 12.2853(11) Å, c = 17.8374(16) Å, V = 3405.2(5) $Å^3$, Z = 4, T = 100(2) K, D_{calcd} = 1.504 g cm^{-3}, μ = 1.377 mm^{-1}, absorption correction factors min. 0.752 max. 0.667, 74355 reflections, 4631 unique (R_{int} = 0.0454), 3948 observed, $R1(F_o)$ = 0.0208 [$I > 2\sigma(I)$], w$R2$ (F_o^2) = 0.0550 (all data), GOF = 1.051. CCDC 2263654.†

Structural data for $[PhTMO]_2[TeCl_6]\cdot 2DMF$ (**2**·2DMF): $[C_{32}H_{50}Cl_6N_4O_4Te]$, M_r = 895.06, yellow block, monoclinic $P2_1/n$, a = 12.5174(4) Å, b = 10.3774(3) Å, c = 15.1349(5) Å, β = 91.9411(12)°, V = 1964.87(11) $Å^3$, Z = 2, T = 100(2) K, D_{calcd} = 1.513 g cm^{-3}, μ = 1.205 mm^{-1}, absorption correction factors min. 0.879 max. 0.812, 59792 reflections, 4890 unique (R_{int} = 0.0178), 4780 observed, $R1(F_o)$ = 0.0174 [$I > 2\sigma(I)$], w$R2$ (F_o^2) = 0.0432 (all data), GOF = 1.064. CCDC 2271363.†

Structural data for $[(p\text{-}CF_3Ph)TMO]_2[TeCl_6]\cdot$(**3**): $[C_{28}H_{34}Cl_6F_6N_2O_2Te]$, M_r = 884.87, yellow prism, monoclinic $C2/c$, a = 19.5893(16) Å, b = 7.4413(6) Å, c = 23.8477(19) Å, β = 90.8384(12)°, V = 3475.9(5) $Å^3$, Z = 2, T = 100(2) K, D_{calcd} = 1.691 g cm^{-3}, μ = 1.379 mm^{-1}, absorption correction factors min. 0.784 max. 0.871, 19515 reflections, 4829 unique (R_{int} = 0.0188), 4499 observed, $R1(F_o)$ = 0.0198 [$I > 2\sigma(I)$], w$R2$ (F_o^2) = 0.0487 (all data), GOF = 1.036. CCDC 2263653.†

Cell cultures. Human pancreatic (PSN-1) and small cell lung cancer (SCLC, H157) cell lines were obtained from the American Type Culture Collection (ATCC, RocKville, MD). The 2008 human ovarian cancer cells were kindly provided by Prof. G. Marverti (Dept. of Biomedical Science of Modena University, Italy).

The LoVo-OXP cells were derived, using a standard protocol, by growing LoVo cells in increasing concentrations of oxaliplatin and following nine months of selection of resistant clones, as previously described.[37]

Cell lines were maintained in the logarithmic phase at 37 °C in a 5% carbon dioxide atmosphere using RPMI-1640 or F-12 culture medium (Euroclone) containing 10% fetal calf serum

(Euroclone, Milan, Italy), antibiotics (50 units × mL^{-1} penicillin and 50 μg mL^{-1} streptomycin), and 2 mM L-glutamine.

MTT assay. The growth inhibitory effect on tumor cells was evaluated by means of the MTT assay.

Briefly, 3–8 × 10^3 cells per well, dependent upon the growth characteristics of the cell line, were seeded in 96 well microplates in growth medium (100 μL). After 24 h, the medium was removed and replaced with a fresh one containing compound **1** at the appropriate concentration. Triplicate cultures were established for each treatment. After 72 h, each well was treated with 10 μL of a 5 mg mL^{-1} MTT saline solution, and following 5 h of incubation, 100 μL of a sodium dodecyl sulfate (SDS) solution in HCl 0.01 M was added. After overnight incubation, cell growth inhibition was detected by measuring the absorbance of each well at 570 nm using a Bio-Rad 680 microplate reader. The mean absorbance for each drug dose was expressed as a percentage of the control untreated well absorbance and plotted *vs.* drug concentration. IC_{50} values, the drug concentrations that reduce the mean absorbance at 570 nm to 50% of those in the untreated control wells, were calculated by the four-parameter logistic (4-PL) model. The evaluation was based on means from at least three independent experiments.

Synthesis

Compound 1. $TeCl_4$ (0.5 g, 1.86 mmol) and pinacol (0.22 g, 1.86 mmol) were added as solids in a round bottomed flask, followed by the addition of dry acetonitrile (6 mL, 114.9 mmol) and reflux for five hours at 80 °C. The yellow solution was then cooled at r.t. and addition of diethyl ether (30 mL) produced a white solid which was recovered by filtration, washed with cold acetonitrile, diethyl ether and dried under vacuum. The solid was re-dissolved in methanol (5 mL) and by addition of water (12 mL) a white solid formed (TeO_2) which was removed by filtration. Subsequently, the filtrate was dried under reduced pressure and the resulting yellow solid was washed with cold methanol (10 mL), diethyl ether (25 mL) and dried under vacuum. Yield: 0.410 g, 70%. Elem. anal. calc. for $C_{16}H_{32}Cl_6N_2O_2Te$, % C: 30.76, H: 5.16, N: 4.48; found C: 30.29, H: 4.94, N: 4.37. ^{1}H-NMR (DMSO-d_6): δ 2.34 (s, 3H, CH_3), 1.49 (s, 6H, CH_3), 1.36 (s, 6H, CH_3). ^{13}C-NMR (DMSO-d_6): δ 173.9 (O–*C*═N), 97.7 (*C*–O), 65.5 (*C*–N), 22.6 (CH_3 pinacol), 22.4 (CH_3 pinacol), 13.9 (*C*H_3). ^{125}Te-NMR (DMSO-d_6): δ 1525. IR [cm^{-1}]: 3215, 2981, 1661, 1490, 1447, 1402, 1379, 1325, 1250, 1166, 1116, 996, 956, 908, 791, 670, 626, 590, 507. LC-MS (*m*/*z*): calculated mass for $(C_8H_{16}NO)^+$: 142.12, found: 142.10.

Compound 2. The procedure for compound **1** was repeated with the difference that acetonitrile was substituted by benzonitrile (6 mL, 58.2 mmol). The yellow solution was then cooled at r.t. and addition of diethyl ether (35 mL) produced a white solid which was recovered by filtration, washed with diethyl ether and dried under vacuum. The solid was re-dissolved in methanol (8 mL) and by addition of water (20 mL) a white solid formed (TeO_2) which was removed by filtration. Subsequently, the filtrate was dried under reduced pressure and the resulting yellow solid was washed with cold methanol (12 mL), diethyl ether (30 mL) and dried under vacuum. Yield: 0.390 g, 55%. Elem. anal. calc. for $C_{26}H_{36}Cl_6N_2O_2Te$, % C: 41.70, H: 4.85, N: 3.74; found C: 41.29, H: 4.54, N: 3.47. ^{1}H-NMR (DMSO-d_6): δ 8.23 (d, 2H), 7.87 (d, 1H), 7.69 (d, 2H), 1.49 (s, 6H, CH_3), 1.36 (s, 6H, CH_3). ^{13}C-NMR (DMSO-d_6): δ 167.0 (O–C═N), 136.1, 129.8, 129.4, 121.2, 97.0 (C–O), 66.6 (C–N), 22.7 (CH_3 pinacol), 22.4 (CH_3 pinacol). ^{125}Te-NMR (DMSO-d_6): δ 1524. IR (cm^{-1}): 2981, 2667, 1629, 1468, 1399, 1378, 1262, 1164, 1141, 1093, 930, 781, 706, 682. LC-MS (*m*/*z*): calculated mass for $(C_{13}H_{18}NO)^+$: 204.14, found: 204.10.

Compound 3. The procedure for compound **1** was repeated with the difference that acetonitrile was substituted by 4-(trifluoromethyl)benzonitrile (5 mL, 37.3 mmol), and the temperature was 75 °C. The yellow solution was then cooled at r.t. and addition of diethyl ether (30 mL) produced a white solid which was recovered by filtration, washed with diethyl ether and dried under vacuum. The solid was re-dissolved in methanol (6 mL) and by addition of water (18 mL) a white solid formed (TeO_2) which was removed by filtration. Subsequently, the filtrate was dried under reduced pressure and the resulting yellow solid was washed with cold methanol (10 mL), diethyl ether (25 mL) and dried under vacuum. Yield: 0.325 g, 39%. Elem. Anal. Calc. for $C_{28}H_{34}Cl_6F_6N_2O_2Te$, % C: 38.00, H: 3.87, N: 3.17; found C: 38.43, H: 4.08, N: 3.58. ^{1}H-NMR (DMSO-d_6): δ 8.24 (d, 2H), 8.00 (d, 2H), 1.52 (s, 6H, CH_3), 1.39 (s, 6H, CH_3). ^{13}C-NMR (DMSO-d_6): δ 165.5 (O–C═N), 134.5, 134.2, 130.5, 126.2, 125.0, 124.5, 122.3 (*C*F_3), 97.1, 67.3, 22.9 (CH_3 pinacol), 22.5 (CH_3 pinacol). ^{125}Te-NMR (DMSO-d_6): δ 1521. IR [cm^{-1}]: 3051, 1637, 1446, 1322, 1263, 1168, 1122, 1096, 1063, 1013, 852, 834, 799, 756, 695, 661. LC-MS (*m*/*z*): calculated mass for $(C_{14}H_{17}F_3NO)^+$: 272.13, found: 272.10.

Author contributions

KDA and TS: investigation, formal analysis, writing – original draft, MDF, VG: investigation, formal analysis. PSM: investigation, data curation, visualization, writing. RR: data curation, visualization, writing, – review & editing. DM: conceptualization, data curation, funding acquisition, project administration, supervision, visualization, writing – original draft, writing – review & editing.

Conflicts of interest

There are no conflicts to declare.

Acknowledgements

This work was supported by Science Foundation Ireland 2012 Strategic Opportunity Fund (Infrastructure award 12/RI/2346/SOF) for NMR facilities, SFI Opportunistic Infrastructure Fund 2016 (16/RI/3399) for LC-MS, the Spanish MCIU/AEI/FEDER (PID2021-122406NB-I00), the Aragón Government (E42_23R) and the University of Zaragoza.

References

1 I. Haiduc, R. B. King and M. G. Newton, *Chem. Rev.*, 1994, **94**, 301–326.

2 A. Silberman, Y. Kalechman, S. Hirsch, Z. Erlich, B. Sredni and A. Albeck, *ChemBioChem*, 2016, **17**, 918–927.
3 H. L. Seng and E. R. T. Tiekink, *Appl. Organomet. Chem.*, 2012, **26**, 655–662.
4 I. A. S. Pimentel, C. de Siqueira Paladi, S. Katz, W. A. de Souza Judice, R. L. O. R. Cunha and C. L. Barbieri, *PLOS ONE*, 2012, **7**, e48780.
5 B. Sredni, *Semin. Cancer Biol.*, 2012, **22**, 60–69.
6 G. M. Frei, M. Kremer, K. M. Hanschmann, S. Krause, M. Albeck, B. Sredni and B. S. Schnierle, *Br. J. Derm.*, 2008, **158**, 578–586.
7 M. S. Silva and L. H. Andrade, *Org. Biomol. Chem.*, 2015, **13**, 5924–5929.
8 B. Sredni, T. Tichler, A. Shani, R. Catane, B. Kaufman, G. Strassmann, M. Albeck and Y. Kalechman, *J. Natl. Cancer. I*, 1996, **88**, 1276–1284.
9 S. Yosef, M. Brodsky, B. Sredni, A. Albeck and M. Albeck, *ChemMedChem*, 2007, **2**, 1601–1606.
10 B. Sredni, R. R. Caspi, A. Klein, Y. Danziger, Y. Kalechman, M. BenYa'akov, T. Tamari, F. Shalit and M. Albeck, *Nature*, 1987, **330**, 173–176.
11 M. Albeck, T. Tamari and B. Sredni, *Synthesis*, 1989, 635–636.
12 A. Albeck, H. Weitman, B. Sredni and M. Albeck, *Inorg. Chem.*, 1998, 1704–1712.
13 E. Okun, T. V. Arumugam, S. C. Tang, M. Gleichmann, M. Albeck, B. Sredni and M. P. Mattson, *J. Neurochem.*, 2007, 1232–1241.
14 Y. Kalechman, U. Gafter, T. Weinstein, A. Chagnac, I. Freidkin, A. Tobar, M. Albeck and B. Sredni, *J. Biol. Chem.*, 2004, 24724–24732.
15 B. Sredni, R.-H. Xu, M. Albeck, U. Gafter, R. Gal, A. Shani, T. Tichler, J. Shapira, I. Bruderman, R. Catane, B. Kaufman, J. K. Whisnant, K. L. Mettinger and Y. Kalechman, *Int. J. Cancer*, 1996, 97–103.
16 B. Sredni, *Semin. Cancer Biol.*, 2012, **22**, 60–69.
17 J. Eskdale, D. Kube, H. Tesch and G. Gallagher, *Immunogenetics*, 1997, **46**, 120–128.
18 H.-L. Seng, H. L. Seng and E. R. T. Tiekink, *Appl. Organomet. Chem.*, 2012, 655–662.
19 K. D'Arcy, A. P. Doyle, K. Kavanagh, L. Ronconi, B. Fresch and D. Montagner, *J. Inorg. Biochem.*, 2019, **198**, 110719.
20 D. Pfaff, G. Nemecekand and J. Podlech, *Beilstein J. Org. Chem.*, 2013, **9**, 1572–1577.
21 K. V. Luzyanin, V. Y. Kukushkin, M. L. Kuznetsov, D. A. Garnovskii, M. Haukka and A. J. L. Pombeiro, *Inorg. Chem.*, 2002, **41**, 2981–2986.
22 A. Guérinot, S. Reymond and J. Cossy, *Eur. J. O. C.*, 2012, 19–28.
23 D. Jiang, T. He, L. Ma and Z. Wang, *RSC Adv.*, 2014, **4**, 64936–64946.
24 J. B. Milne, *Can. J. Chem.*, 1991, **69**, 987–992.
25 F. A. Jerca, V. V. Jerca and R. Hoogenboom, *Biomacromolecules*, 2021, **22**, 5020–5032.
26 R. Greenhalgh, R. M. Heggie and M. A. Weinberger, *Can. J. Chem.*, 1963, **41**, 1662–1670.
27 G. P. Moloney, M. N. Iskander and D. J. Craik, *J. Pharm. Sci.*, 2010, **99**, 3362–3371.
28 M. P. Rigobello, A. Folda, A. Citta, G. Scutari, V. Gandin, A. P. Fernandes, A.-K. Rundlöf, C. Marzano, M. Björnstedt and A. Bindoli, *Free Rad. Biol. Med.*, 2011, **50**, 1620–1629.
29 M. P. Rigobello, A. Folda, A. Citta, G. Scutari, V. Gandin, A. P. Fernandes, A.-K. Rundlöf, C. Marzano, M. Björnstedt and A. Bindoli, *Free Rad. Biol. Med.*, 2009, **47**, 710–721.
30 V. Gandin and A. P. Fernandes, *Molecules*, 2015, **20**, 12732–12756.
31 SAINT+, version 6.01: Area-Detector Integration Software; Bruker AXS: Madison, WI, 2001.
32 SADABS, Area Detector Absorption Program; Bruker AXS: Madison, WI, 1996.
33 L. Krause, R. Herbst-Irmer, G. M. Sheldrick and D. Stalke, Comparison of Silver and Molybdenum Microfocus Xray Sources for Single-Crystal Structure Determination, *J. Appl. Crystallogr.*, 2015, **48**, 3–10.
34 G. M. Sheldrick, A Short History of SHELX, *Acta Crystallogr.*, 2008, **64**, 112–122.
35 G. M. Sheldrick, SHELXT – Integrated Space-Group and Crystal-Structure Determination, *Acta Crystallogr.*, 2015, **A71**, 3–8.
36 L. J. Farrugia, WinGX and ORTEP for Windows: an Update, *J. Appl. Crystallogr.*, 2012, **45**, 849–854.
37 V. Gandin, M. Pellei, F. Tisato, M. Porchia, C. Santini and C. Marzano, *J. Cell. Mol. Med.*, 2012, **16**, 142–151.